Progress on Phase Separation Microfluidics

Damena D. Agonafer, James Palko, Yoonjin Won, Ken Lopez, Tom Dusseault, Julie Gires, Mehdi Asheghi, Juan G. Santiago, Kenneth E. Goodson

Mechanical Engineering Department, Stanford University, Stanford, CA 94305

***Abstract* — High power density GaN HEMT technology can increase the capability of defense electronics systems with the reduction of CSWaP. However, thermal limitations have currently limited the inherent capabilities of this technology where transistor-level power densities that exceed 10 kW/cm^2 are electrically feasible. This paper introduces the concept of an evaporative microcooling device utilizing some of the current two-phase vapor separation technologies currently being developed for water and dielectric liquids.**

***Index Terms*— GaN, HEMT, Electronics Cooling.**

I. Introduction

Dimensional scaling and corresponding exponential increase in transistor density has been accompanied by a significant increase in power density in microchips and the heat flux for high performance chips in the 14 nm generation is projected to be greater than 100 W/cm^2 with a junction-to-ambient thermal resistance <0.2°C/W [1]. High power density GaN high-electron-mobility transistor (HEMT) technology can increase the capability of defense electronics systems however, thermal challenges arise due to transistor-level power densities that can exceed 10 kW/cm^2. This has motivated research on liquid cooling, both direct [2] and indirect [3], have been well with an emphasis on addressing challenges for high power electronics and reducing cost related to the system level integration.

In this work, we focus on developing vapor phase separation technology designed for an evaporative microheat exchanger, designed to target heat fluxes exceeding 5 kW/cm^2 with a temperature rise of less than 5K. To achieve these aggressive targets, three essential goals must be met: 1.) Obtaining a stable, ultra-thin evaporating liquid film at the walls of the microcooling device that remains wetted even at extreme heat fluxes and does not flood at low heat fluxes. 2.) Providing adequate liquid delivery and vapor extraction while maintaining small pressure drops (to minimize elevation of saturation temperature and required pumping power). 3.) Ensuring the lowest possible thermal conduction and convection resistances from heat generation volumes to the phase change surface including conduction along extended surfaces. We address these issues with a tightly integrated combination of porous material design, surface engineering, intricate microfluidic phase management, and application of available materials with exceptional thermal properties but major integration challenges. Chemical and geometric surface engineering is being applied for robust and finely controlled phase separation including advances in fundamental understanding of effects of geometrically optimized surfaces for retaining completely wetting liquids,

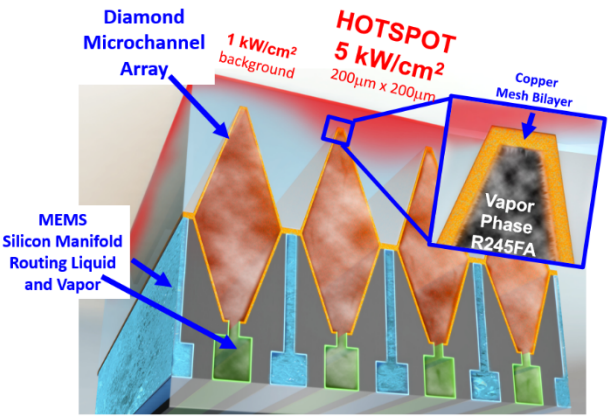

Fig. 1. Schematic of our microcooling heat exchanger device used to remove heat fluxes exceeding 5 kW/cm^2. The microcooling technology includes diamond fin channels for heat spreading integrated with and a thin microporous copper layer and bilayer for evaporative cooling and phase separation.

such as dielectric refrigerants. Finally, all these elements are being integrated with high thermal conductivity substrates including diamond. Figure 1 shows a schematic of our microcooling heat exchange device. Heat is spread from the hot spot to the diamond fins, where liquid is delivered through a thin microporous copper liquid delivery layer that allows evaporative cooling at the top of the nanoporous capping layer. Phase separation occurs by integration of a nanoporous cap layer (bilayer) that extracts vapor and retains liquid by maintaining a capillary pressure that exceeds the viscous pressure loss across the microporous copper layer. Evaporative cooling is maintained at the top of the liquid delivery layer while boiling is suppressed by maintaining a liquid pressure greater than the saturation pressure.

978-1-4799-3622-9/14/$31.00 ©2014 IEEE

II. VAPOR PHASE SEPARATION TECHNOLOGY

A. Study of Key Parameters for Microporous Copper Liquid Delivery Layer and Bilayer

As previously discussed, it is critical to design a phase separation device that maintains capillary pressures exceeding the viscous pressure drop across the microporous layer in order to mitigate flooding at the bilayer's top surface and suppress boiling. We therefore, simulate the key parameters for minimizing both the thermal and hydrodynamic resistances.

The bilayer and liquid delivery layer is integrated on a diamond fin of 5000 μm x 500 μm. The working fluid used in these studies is R1234ze. The viscous pressure drop across the microporous layer is calculated based on a 2D Darcy Model using COMSOL Multiphysics as a function of pore diameter, porosity, and tortuosity. The permeability constants are calculated using the Kozeny-Carman equation, where porosity (□)=0.7, grain size (d)=1-20 μm, and tortuosity (τ)=1.1. The boundary conditions

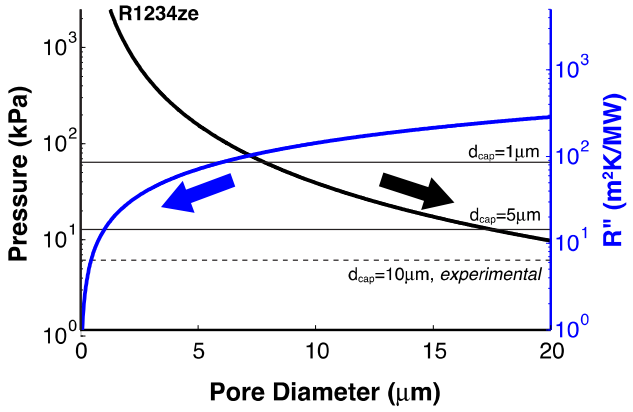

Fig. 2. Pressure drops for various pore diameters are calculated using COMSOL Multiphysics simulation. This figure shows burst pressure limits with various capping layer pore diameters from 1 μm to 10 μm. Thermal resistance (R"=1/h) has been scaled as $1/h=d/k$ where k and d are the effective thermal conductivity and pore diameter, respectively.

include a pressure inlet and evaporative mass generation out of plane, where mass flux is calculated based as the heat flux and latent heat of the working fluid. All other sides of the microporous layer are considered adiabatic.

The viscous pressure across the microporous copper layer drop is plotted as a function of pore diameter as shown in Fig. 2. The plot shows smaller pore sizes yield smaller convective resistances (*i.e.* larger surface to area to volume ratio) but at the expense of higher viscous pressure drops. A pore size of 1 μm leads to a pressure drop of ~60 kPa across the microporous layer, which requires the bilayer to have a pore size ~1 μm in order to yield a burst pressure that matches the viscous pressure drop.

B. Vapor Pressure Drop Analysis across Bilayer

Small pore sizes for the bilayer is advantageous because it increases the bursting pressure, thus allowing the capabilities of liquid to be delivered at higher pressure through the microporous layer, while mitigating flooding at the top of the bilayer. However, reducing the pore size decreases the capability of the membrane to transport vapor. The hydrophobic capping layers are dry, with the evaporating surface maintained below them. Therefore, the bilayer must allow the passage of large volumetric flow rates of vapor.

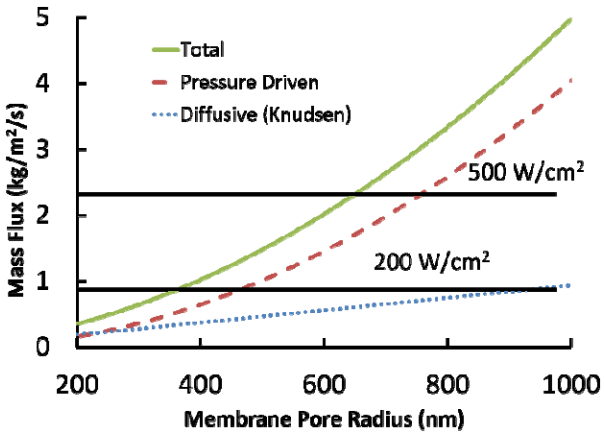

Fig. 3. Pressure drop across a hydrophobic nanoporous capping layer for an applied heat flux

We have modeled the ability of a nanoporous layer to transport vapor from the evaporating surface due to diffusive and pressure driven transport [4]. These two fluxes have different dependencies with pore radius. Figure 3 shows the mass flux and its contributions due to pressure driven flow and diffusion as a function of pore size across a 10 μm thick membrane with a driving pressure difference of 10 kPa for water at 393K. The evaporative surface is assumed to be at saturated conditions. Porosity and tortuosity of the membrane are 0.75 and 2 respectively. Horizontal lines indicate mass fluxes required to support heat fluxes of 200 W/cm^2 (0.9 kg/s/m^2) and 500 W/cm^2 (2.3 kg/s/m^2). We can see that the mass flux sustained by the membrane is sufficient to support extreme evaporative cooling applications.

C. Optimized Pore Geometry for Dielectric Liquids

Dielectric fluids exhibit wetting properties that do not allow for feasible chemical surface modifications for producing non-wetting surfaces, such as with hydrophobic surfaces used with water. Hence, this leaves the design of a phase separation membrane to rely solely on geometric considerations. In order to successfully produce the necessary capillary burst pressures for phase-separation, the pore-level geometries must exhibit a sudden sharp discontinuity in their shapes [5].

Figure 4 shows burst pressure experiments performed using microglass capillaries. Initially flow encounters minimal viscous effects as the flow rate is maintained well

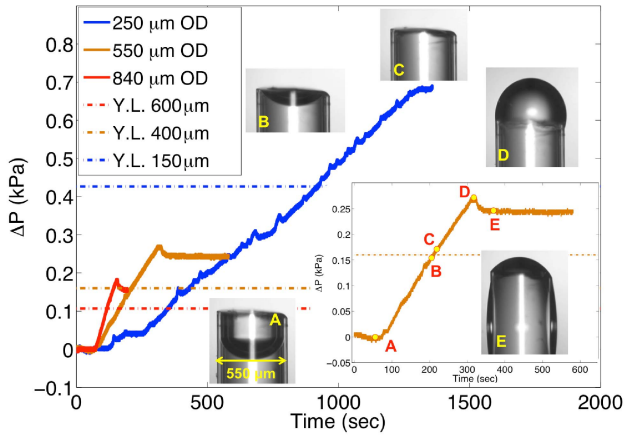

Fig. 4. Glass capillary bursting pressure experimental results for FC-40.

below the regime where viscous effects are significant ($Ca<10^{-5}$), and consequently, the pressure remains constant (point A in Fig. 4.). During this period, the pressure in the liquid is lower than that in the gas above by an amount determined by the curvature of the meniscus as it climbs up the capillary. At this point, the pressure in the liquid begins to rise as the meniscus becomes less concave (point B, Fig.4.). Eventually, the meniscus becomes planar, and the pressure between the liquid and gas phases is equal as shown at point C in Fig. 4. The meniscus runs off to the outer diameter edge of the microglass capillary, where it pins and begins to grow in curvature. The meniscus is able to reach the surface of the outer diameter where it reaches its minimum radius of curvature and maximum burst pressure, which is indicated at point D in Fig. 4. After the burst pressure is reached, viscous and evaporative effects balance the capillary flow forces which gives a constant pressure plateau as seen at point E in Fig. 4. These results show proof that a microfabricated structure can be engineered to 'pin' dielectric liquids based on optimization of pore geometry.

III. MATERIAL FABRICATION FOR BILAYER

A. Fabrication of Microporous Copper Layer

Resistance to heat conduction across thin liquid films has posed a classic problem for liquid cooling technologies. Liquid film thickness on the order of microns is required for management of next-generation heat fluxes on the order of 10 kW/cm^2 with feasible pumping requirements. To address this issue, we are developing thin porous copper films to deliver fluid to hotspots.

We fabricate thin porous copper films using the colloidal template method described in previous work [6]. Figure 5 summarizes the steps involved for fabrication of the copper microporous liquid delivery layer. The first step includes synthesizing monodisperse polystyrene spheres with diameters on the order of 1 μm using dispersion polymerization. The template is fabricated for the porous material by drop casting a suspension of spheres in ethanol on silicon wafers with Ti/Au seed layers deposited

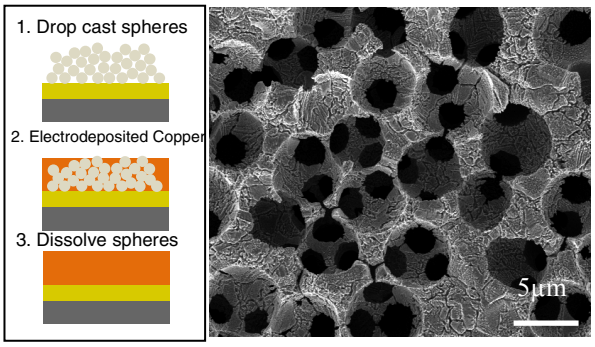

Fig. 5. Fabrication steps for porous copper films using the colloidal crystal template method (left) and top view SEM image of porous copper (right).

by physical vapor deposition (PVD). Following metallization of the silicon substrate, copper is electrodeposited through the bed of packed spheres. The polymer spheres are then dissolved using in tetrahydrofuran (THF) in order to attain the microporous copper structure. This method allows the growth of porous thin films of thickness on the order of 10 microns. We characterize the porosity of the porous copper films by analyzing cross-sectional scanning electron micrographs as described in previous work [6]. Our samples typically have porosities in the range of 60-90%.

B. Fabrication of a Hydrophobic Capping Layer

For water, the key element in producing capping layers with high burst pressures that impose a specific phase boundary is achieving strongly hydrophobic surface chemistries along with fine pore sizes. We have developed monolithic porous layers of hydrophobic material to accomplish these goals. Monolithic layers allow ease of localization and independent control of pore size and porosity, since they are deposited as a separate layer on top of the microporous layer. Monolithic phase separation layers, however, also pose challenges. Bonding is less robust, as the burst pressure is supported by a sharp interface at the top of the microporous layer, and thickness of the layer must be tightly controlled so as not to excessively impede the escape of vapor.

We use phase separation to produce monolithic hydrophobic capping layers composed of polyvinylidenefluoride (PVDF) based on their successful application in microfluidic gas/liquid contactors [7]. Figure 6 shows an example of the layers produced. The fabrication process consist of: 1.) dissolution of PVDF (20 wt%) in dimethylacetamide (DMAc) 2.) casting of films from the PVDF/DMAc solution 3.) rapid immersion of the cast films in a second liquid which is miscible with DMAc but does not dissolve PVDF (e.g. 1:1 ethanol:water).

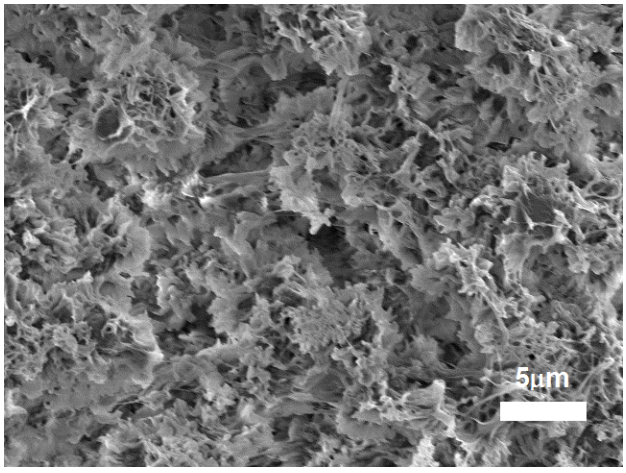

Fig. 6. Nano-porous PVDF produced by phase separation from solution.

Spin coating or doctor blading can be used to deposit the PVDF solution. Thicknesses of ~10 μm have been achieved with targeted thicknesses as small as 1 μm. Immersion of the film results in rapid removal of DMAc from the PVDF solution and the formation of porous, solid PVDF, with submicron pore sizes.

V. CONCLUSION

We have developed phase separation technologies in order to mitigate the challenges with pressure drops associated with two-phase liquid cooling. We are applying these advances to next generation power devices such as microwave high-electron mobility transistors (HEMT) and ultra-high density chip scale integrated (stacked chip) digital devices such as microprocessors. By attacking the fundamental limitations to electronics cooling, we have the opportunity to deliver orders-of-magnitude gains in heat flux removal and open up dramatic avenues of advance for application of electronic devices.

ACKNOWLEDGMENT

The authors would like to acknowledge financial support from DARPA (agreement # HR0011-13-2-0011, titled: Phase Separation Diamond Microfluidics for HEMT Cooling) monitored by Dr. Avi Bar Cohen, Dr. Joe Maurer, and Dr. Matin Kaiser.

REFERENCES

[1] H. Graeb, "ITRS 2011 analog EDA challenges and approaches," in *Design, Automation & Test in Europe Conference & Exhibition (DATE), 2012*, 2012, pp. 1150-1155.

[2] M. Arik and A. Bar-Cohen, "Immersion cooling of high heat flux microelectronics with dielectric liquids," in *Advanced Packaging Materials, 1998. Proceedings. 1998 4th International Symposium on*, 1998, pp. 229-247.

[3] R. C. Chu, U. P. Hwang, and R. E. Simons, "Conduction Cooling for an LSI Package: A One-Dimensional Approach," *IBM Journal of Research and Development,* vol. 26, pp. 45-54, 1982.

[4] R. Schofield, A. Fane, and C. Fell, "Heat and mass transfer in membrane distillation," *Journal of membrane Science,* vol. 33, pp. 299-313, 1987.

[5] D. D. Agonafer, Lopez, K., Palko, J., Won, Y., Asheghi, M., Santiago, J.G., Goodson, K.E., "Phase-Separation of Wetting Fluids Using Nanoporous Alumina Membranes and Micro-GLASS Capillaries," in *IEEE Intersociety Conference on Thermal and Thermomechanical Phenomena in Electronic Systems (ITHERM)*, Orlando, Fl, 2014.

[6] T. J. Dusseault, Gires, J., Barako, M.T., Won, Y., Agonafer, D.D., Asheghi, M., Santiago, J.G., Goodson, K.E., "Inverse Opals for Fluid Delivery in Electronics Cooling Systems," in *IEEE Intersociety Conference on Thermal and Thermomechanical Phenomena in Electronic Systems (ITHERM)* Orlando, Fl, 2014.

[7] E. Karatay and R. G. Lammertink, "Oxygenation by a superhydrophobic slip G/L contactor," *Lab on a Chip,* vol. 12, pp. 2922-2929, 2012.